Atmósfera (2001) 14, pp. 171-188

Ozone distributions in Mexico City using principal component analysis and its relation to meteorological parameters

DIETER KLAUS, ANDREAS POTH, M. VOSS

Institute of Geography, University of Bonn, Germany

ERNESTO JAUREGUI

Centro de Ciencias de la Atmósfera, UNAM, Circuito Exterior, CU, 04510, México, D. F.

(Manuscript received, Sept. 12, 2000; accepted in final form Jan. 25, 2001)

RESUMEN

Se hace una descripción de los patrones de O_3 y su relación con algunas variables meteorológicas (temperatura, vientos superficiales y radiación global). Las observaciones se expresan en términos de eigenvectores y sus coeficientes asociados con el fin de determinar los rasgos generales de los patrones espaciales de ozono. Utilizando los datos simultáneos de los vientos dominantes a una altura de 700 hPa fue posible dar una explicación de algunas distribuciones características del O_3 sobre la Ciudad de México. En el presente estudio se ha intentado proporcionar un conocimiento adicional de la distribución del ozono y su relación con algunos parámetros meteorológicos en la zona metropolitana de la cuenca de México.

ABSTRACT

A description is made of ozone patterns as related to some meteorological variables (temperature, surface wind direction, speed, and global radiation). The observations are expressed in terms of eigenvectors and their associated coefficients in order to determine the gross features of the ozone city-wide patterns. By using concurrent 700 hPa prevailing upper winds and the observed converging surface winds induced by local and regional currents it was possible to provide a physical explanation for some characteristic ozone distributions observed in the MCMA. The present study attempts to provide additional basis to the knowledge of relationships between ozone distributions and meteorological parameters in the Mexico Basin.

1. Introduction

Urban populations in large metropolitan areas suffer from the adverse long-term effects on their health from air pollution. This is particularly true in cities of Eastern Europe, Southeast Asia, Africa and Latinamerica (WHO, 1997). Mexico City is well known for its badly polluted atmosphere. Ozone, one of the most serious offenders to health, was still above the WHO accepted standard on 300 days in 1999. Not withstanding the above situation, some signs of improvement in air quality are beginning to appear. In 1990 to 1992 pollutants (mainly ozone) hit emergency levels on as many as 177 days per year. During 1999, even after a stricter threshold had been introduced the year before, ozone triggered emergencies on just five days (Office of the Environment Annual Report 1999). The achievement suggests, as noted by Smith (2000) that, even Third World cities can begin to reduce air pollution if they seriously have the will to do so. Improvement in air quality in 1999 resulted in a reduction of eye and bronchial illnesses placing less demand on medical services and hospitals according to the city's Ministry of the Environment report.

While population increase in Mexico City was high up to the 1980s (well above two percent, Ezcurra and Mazari, 1996) it leveled off during the 1990s and is presently estimated to be composed of 8.5 million living in the Federal District plus 10 million more inhabitants settled in the metropolitan area. The city is located in the southwestern portion of a broad elevated basin 7500 km2 in extension, the urban area sprawls over 1500 km2. Volcanic ranges surround the ancient lacustrine plains on the east, south and west. To the north the basin is surrounded by discontinuous lower ranges. The encircling mountains restrict horizontal ventilation and thus are a major cause for the confinement of air pollution. The prevailing weak winds and frequent thermal inversions during the cool season favor the high levels of pollution during this period.

The accelerated rate of urbanization in this megacity has led to changes in the thermal, humidity and health conditions in the basin (Oke *et al.*, 1999; Jáuregui and Tejeda, 1997). Emissions from 3000 industries, and about 4.3 million vehicles burning some 44 million liters of fuel per day not infrequently produce above-standard concentrations of nitrogen oxides, which are the main precursors for ozone. (Ceballos, 1998). A contributing factor for the high O_3 precursor emissions is the high elevation of the city and the resulting reduction in oxygen promoting incomplete combustion of gasoline in old vehicles (Collins and Scott, 1993).

Processes leading to ozone generation and distribution in the Mexico basin have been profusely studied in an effort to predict critical pollution scenarios with the purpose of protecting the population. By using modeling techniques Bossert, 1997; Fast and Zhong, 1998a; Williams *et al.*, 1995 have concluded that ozone transport and dispersion is the result of the interaction between local, regional and synoptic circulations.

Dispersion and transport of ozone in the Mexico City Metropolitan Area MCMA have been the object of considerable investigations (Bossert, 1997, Fast and Zhong, 1998b; Williams *et al.*, 1995). Results from model simulations show that both local and regional synoptic flows determine the observed temporal and spatial ozone concentrations. Data from the MARI research programe to investigate the air quality problem in the MCMA (see Nickerson *et al.*, 1992) have been used to define local meteorological and air quality conditions in order to gain insight in the interaction between synoptic, regional and local circulations as well as in the dynamics and structure of the boundary layer (Fast and Zhong, 1998a; Whiteman *et al.*, 2000). Doran and Zhong (1999), were able to show that for example the so called gap winds were relevant in relation to the spatial distribution of ozone in the MCMA.

The purpose of this study is in the light of the above new findings, to describe, classify and explain, the temporal and spatial variations of ozone distributions in the Mexico Basin for the year 1995 in relation to their dependence on some meteorological variables.

2. Method

The statistical technique used for this purpose in this study is the eigenvector analysis. This approach allows to objectively determine the most significant ozone patterns in terms of the variance of the original observations explained by each pattern. This method was applied in early studies by Blifford and Meeker (1967) and Peterson (1970; 1972). One property of the eigenvector technique that makes it advantageous

for describing the gross features of the pollutant patterns over an urban area, is that it smoothes or partially filters the observations (Peterson, 1970). According to this author, the patterns de-emphasize very localized, extreme values of a pollutant, which occurs frequently, whereas they emphasize the large-scale frequently occurring distributions. In recent times quite a number of studies have attempted to elucidate ozone and other pollutants dependence on meteorology using principal component analysis methodology (Harrison, 1997; Statheropoulos *et al.*, 1998; Beceiro *et al.*, 1998; Lam and Cheng, 1998).

3. The data

Air quality and meteorological data from a network of 15 stations were available for period February to December, 1995. Figure 1 shows the location of monitoring stations operated by RAMA (Automatic Atmospheric Monitoring Network) from the city's Office of the Environment (D. G. P. C. C., 1995).

Hourly values of ozone (in ppm) for 15 stations and hourly temperature and wind for 12 sites were analyzed. Data from stations Minería and Texcoco were available from the Centro de Ciencias de la Atmósfera, UNAM, México. All data were tested for homogeneity. In those cases where values were defective or missing they were substituted for new estimates using correlation methods.

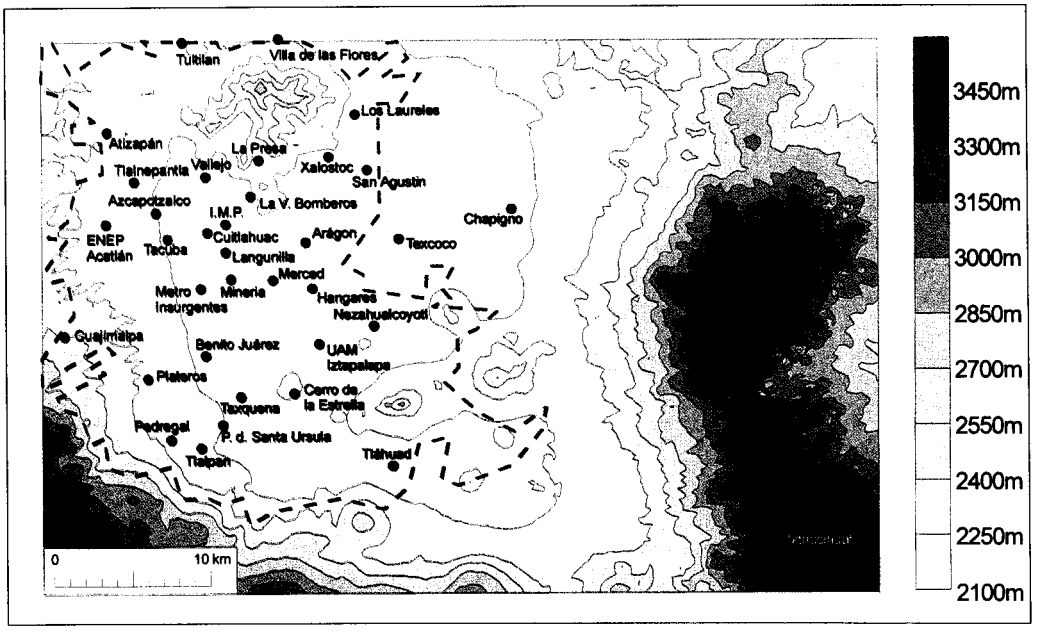

Fig. 1. Mexico City Metropolitan Area (MCMA) and location of stations.

4. Mean air circulation conditions in the MCMA

Figure 2a shows the mean hourly wind vectors for the dry season in 1995. The stations are ordered from northwest (Tlalneplantla) to south (Pedregal) and then to the center-east (Estrella) ending in the northeast corner of the urban area (Xalostoc).

In stations to the west from 0-8:00 and at night (from 21:00 to 0:00) light winds blow from the west northwest shifting to north in the afternoon with increasing intensity. Maximum windspeeds occur around 18:00-19:00 hours. These winds illustrate the daily cycle of the thermally-driven mountain/valley wind circulation that in the afternoon and early evening are modified by strong convection and transport from upper level (700 hPa) wind impulse from the south or from the west.

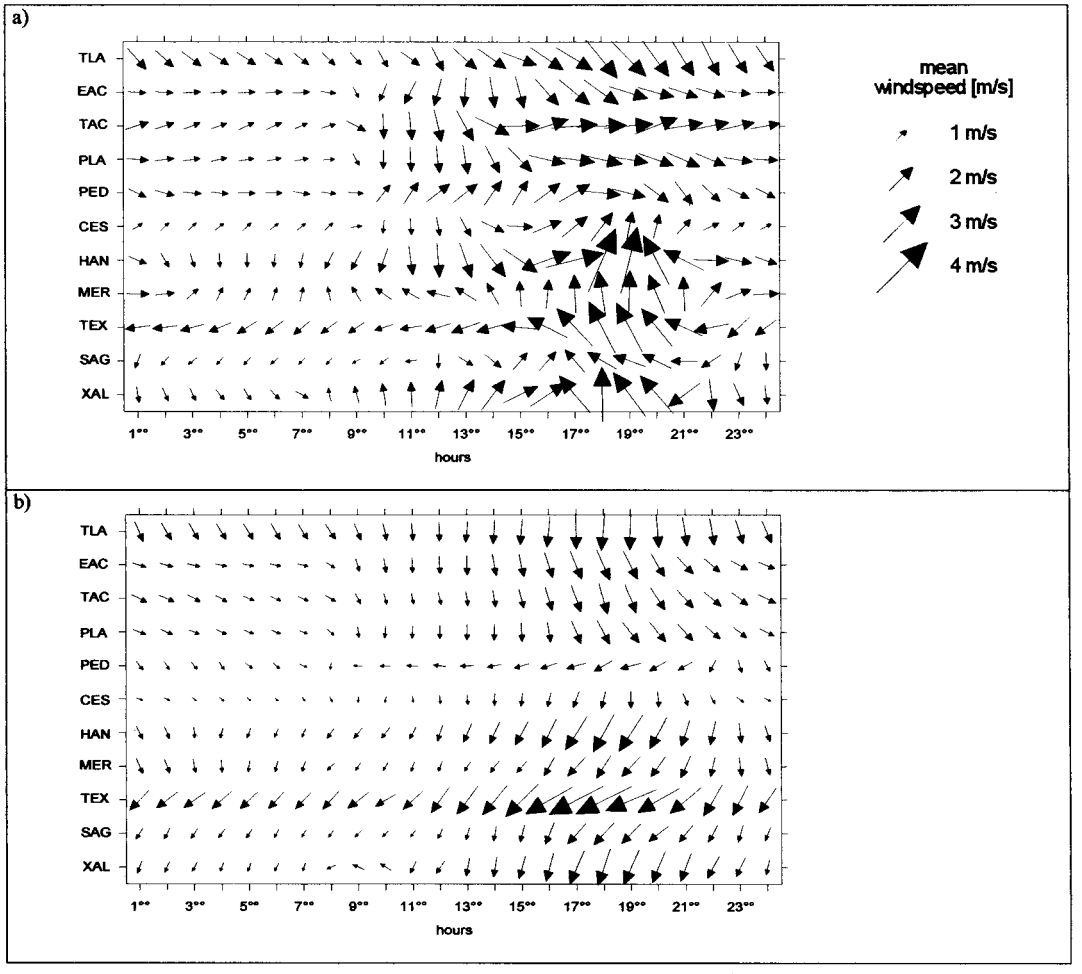

Fig. 2. Mean daily hourly variation of surface winds during the dry season (a) and rainy season (b) months for year 1995 and at stations Tlanepantla (TLA), ENEP Acatlán (EAC), Tacuba (TAC), Plateros (PLA), Pedregal (PED), Cerro Estrella (CES), Hangares (HAN), Merced (MER), Texcoco (TEX), San Agustín (SAG) and Xalostoc (XAL).

Stations located in the center and on the eastern side, show a different wind pattern during the dry season. At night the cool drainage winds show various directions with prevailing northwest winds. Central station Merced shows weak southerly winds that are reinforced in the early evening by, cool-down-the-mountain flow from the south.

During the day on the eastern portion of the plain, east component winds dominate until about mid afternoon. After about 16:00 southerly winds begin to blow with increasing intensity reaching a peak between 17:00-21:00 hours (Fig. 2a). The above described winds blowing from the west northwest on the western side of the urban area and those flowing from the southern direction on the eastern side of the basin result in a converging cyclonic flow in the late afternoon and early night which is reinforced by the centripetal flow generated by the heat island of the urban area (Klaus *et al.*, 1999).

During the morning hours (9:00 to 12:00) upper winds from the south are in 60% of the observations related to strong northerly surface winds on the western side of the basin. The pollutant-laden air mass moving from north to south in the lower levels flows upslope the mountains to the south and then turns northwards by the upper level southerly wind current ending its trajectory on the lower levels by vertical diffusion. Simultaneously the mixing layer grows from less than 0,5 km up to 2-4 km depth in the afternoon in connection with an intense vertical transport of momentum as evidenced by the velocity maximum of the observed surface winds during the late afternoon.

The surface northerly and southerly winds during the day-time hours of the dry season are the result of the temperature contrast between the basin and the free atmosphere in an altitude of 2200 m reaching 1-2°C/km (Newell *et al.*, 1972; Doran and Zhong, 1999). The opening of the basin to the north favors the creation of a thermal-induced surface north current. Simultaneously occurring winds aloft from the south have a frequency of 38% during the dry season. Between the south winds aloft and the frequent surface thermally-driven winds from the north there is a shear layer that modifies the surface northerly current. When both, overlying winds aloft and surface winds blow from the north the latter reach maximum intensity.

Upper level winds from the south favor the creation of thermal southerly surface winds by decelerating the surface north winds. This deceleration of the surface northerly current is evident on the southeastern corner of the basin around Amecameca. Only in the late afternoon hours do these weakened surface currents invert their direction and pick up speed and peak (Fig. 2a). When east and north winds prevail aloft, the surface southerly winds appear rarely (10-15%), whereas when west and south west winds dominate aloft the frequency of low-level southerly winds increases to 55-75% on the eastern side of the basin.

As a result of the daily variations of the mixed layer depth the winds at the 700 hPa level undergo daily variations too. During the dry season upper westerlies occur in 73% of all cases at 6:00 a.m. and in 27% at the 18:00 hours sounding. It is only when both upper and lower circulations are uncoupled during the night, when the undisturbed synoptic westerlies prevail. For the upper level east winds the frequencies are reversed: 73% at 18:00 and 27% at 6:00 hours. Upper level south winds at both hours have a frequency of 50% while northerly winds aloft show a frequency of 60% at 18:00 hours and 40% in the morning sounding.

These changes in the wind direction at 700 hPa illustrate the influence the local and regional east and north surface winds have on the currents aloft as a result of the vertical development of the mixed layer (Fast and Zhong, 1998a; Whiteman *et al.*, 2000; Klaus *et al.*, 1999). During the night the developing surface inversion decouples the surface wind field from the winds at 700-hPa level where the synoptic winds prevail.

Figure 2b shows the mean hourly wind vectors during the wet season months of May to October 1995. Surface wind directions during the night show the cool air drainage flow. This pattern of weak winds from the west on the western portion of the basin, is substituted by northwest winds during daytime hours and on the eastern part of the plain by north, northwest winds. On the eastern side of the basin the dry-season southerly winds occurring during the late afternoon hours are substituted by a more homogeneous stream from the northeast in the wet season.

From the above results a simple circulation scheme for the Mexico basin arises (Whiteman *et al.*, 2000; Klaus *et al.*, 1999; Fast and Zhong, 1998a; Jauregui, 1997; Bossert, 1997): during the night and early morning hours an intense heat island develops over the urban area. The converging centripetal circulation (or rural winds) are reinforced by the drainage cool winds from the surrounding mountains. The boundary layer is expanded during this time to about 100 m. In the course of the morning and early afternoon the intense solar radiation, particularly during the dry season, generates a sudden increase of the mixed layer to up to 2-4 km above ground level reaching maximum vertical expansion in the region of upslope flow.

Pollutants carried by the upslope winds into the south and west winds aloft, are moved to near-surface levels by downward diffusion in the early afternoon hours. During this time the heating of the air mass contained in the basin can generate a compensating surface flow from the north direction on the west side of the basin and a south current on the eastern portion of the basin, especially when a flow from the south prevails aloft.

The flow from the south reaches the basin in the afternoon hours along the Cuautla-Amecameca-Chalco corridor. In late afternoon this south current sometimes flows toward the northern flanks of the Ajusco range generating a converging circulation over the urban area of the MCMA. This converging air mass flow intensifies the vertical extension of the mixed layer. In this way the polluted air is carried to higher levels where it is transported away from the basin by the upper wind current.

The above described situation changes with the season. From May to October the upper level winds blow from the north and east 60% of the time. During the rest of the year winds from the south and west prevail. The winds from the east and north are mainly related to moisture laden air masses from the Gulf of Mexico, leading to the formation of convective clouds which precipitate in the form of rain showers. From November

to April the basin is under the influence of the upper-level westerly current from temperate latitudes. The occasional front passages of cold air masses are seldom linked to convective clouds and light rain. Most of the dry season is characterized by anticyclonic clear weather (Klaus *et al.*, 1999).

5. Daily variations of ozone concentration

For both, rainy and dry season, the mean daily variation of ozone concentration peaks in the early afternoon soon after maximum temperature and irradiation occur (Fig. 3a). Minimum ozone values are observed during the night. Southern station Pedregal (PED) shows the highest ozone concentration, station Merced (MER) in the city center shows an intermediate value whereas the lowest mean daily concentrations are observed at the northern station Tlanepantla (TLA). Moreover, maximum ozone concentration occurs in the southern basin (PED) one hour later than in the central (MER) and northern part (TLA). During the night, the highest concentrations are observed in Tlanepantla (TLA), the lowest in Merced (MER). In the morning hours until 11.00 the highest ozone concentration occurs in the central part of the city (MER), in the afternoon and early night hours the lowest concentrations are observed here (Fig. 3a).

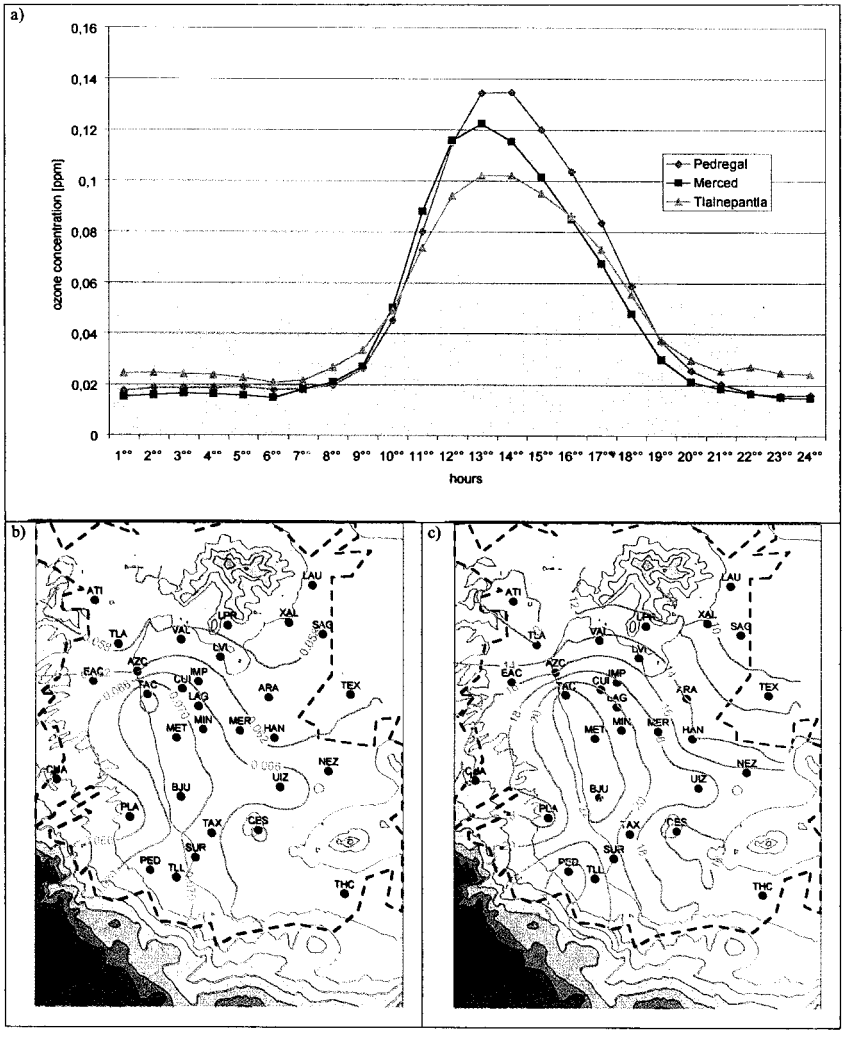

Fig. 3. Mean hourly ozone concentration in ppm (parts per million) for stations Pedregal, Merced and Tlanepantla during the period from February to December 1995 (a). Mean hourly ozone concentration from 8:00-20:00 hours for year 1995 (b). Frequency of exceedances (%) of mean hourly ozone concentrations above the local standard (c) for Mexico City (0.11ppm).

The spatial distribution of the mean ozone concentrations for the day time hours (8-20.00) of year 1995 are shown in Figure 3b. The highest ozone concentration can be observed in the vicinity of the southwestern and western mountain slopes, the lowest in the northern and eastern part of the basin. The highest mean concentrations in the south remain under 0.07ppm, quite below the hourly standard for ozone in Mexico (0.11 ppm). Figure 3c shows that on the south western corner the standard is exceeded 24% of the hourly observations but only 10% towards the northeast during the period 8:00-20:00 hours.

The mean circulation conditions during the dry season described in the preceding section favor a north-south pollutant transport towards Pedregal station (PED) and beyond. In the dry season during the afternoon surface winds from the north converge with surface winds from the south and southeast in the southern and central part of the basin. During the rainy season there exists a convergence between the northern surface winds in the western and the northeastern and eastern surface winds in the eastern part of the basin. This air mass convergence explains the high ozone concentrations on the western and central parts of the area and also the appearance of the ozone maximum at Pedregal (PED) around one hour later as compared with stations further north. Moreover, during the morning before 11:00 hour ozone values are higher in the city center (MER) than those observed in the south at Pedregal (Fig. 3a).

During the dry season pollutants that are carried by the upslope winds are infiltrated into the dry-season upper southwest winds and can return by vertical diffusion down to near-surface levels in the western and central parts of the basin. Due to the washout effect these processes play a minor role during the wet season.

6. Evaluation of typical space distributions of ozone

The increase of the north-south transport of the ozone-loaded air mass depends on the space distribution of precursor emissions. In order to better evaluate this dependence there is a need to identify the typical space ozone distribution and its variation with time. This may be accomplished by using the principal component analysis PCA. This method is described by Skaggs (1975) and is also known as Empirical Orthogonal Functions (EOF).

The PCA is based on the study of the hourly ozone values from February to December 1995 for 15 stations. Since the high ozone concentrations representing a high risk to health occur during the daytime hours (Fig. 3a) the analysis is made only from 8:00 to 20:00. We obtained 4342 values (334 days x 13 hours) for each of the 15 station.

Ozone distributions from similar space samples of a principal component are represented by an eigenvector in such a way that the hourly ozone distributions correspond with the 4342 components from the extracted eigenvector showing high positive or negative values. The partial variance explained by one eigenvector explains the significance of the sample with respect to the other space samples.

Figures 4a-d show the distributions of the coefficients for the first four eigenvectors which explain 54.2% of the total variance. The four series of the 4342 components of these eigenvectors correspond to the mean daily cycles (Fig. 4e). The display of further eigenvectors shows that the portion of the explained variance is relatively small and that the space distribution of the coefficients only determines small gradients.

The four space distributions of the eigenvectors coefficients are very clearly differentiated (Figs. 4a-d). Each of the 4342 extracted components correspond to the real ozone distributions for a particular hour. The bigger the value of the respective eigenvectors component at that hour, the more similar is the real ozone distribution and the spatial pattern of the coefficients.

For the first eigenvector the components receive maximum values at 12:00 hours; for the second around 14 hours; for the third around 19:00 and for the fourth at 11:00 hours. The pattern of the coefficients occurring on these hours explains only the relative spatial distributions of the real ozone concentrations. Moreover, it is not possible to make a statement on the persistence of the samples.

These disadvantages may be removed by actually adding ozone concentration values at each station where the components of the eigenvectors show high positive or negative values. In this study, only those hours in which the eigenvectors component values are higher or smaller that $\pm$ 1.5 sigma are considered. Sigma is computed with respect to the 4342 components of the corresponding eigenvectors. The mean hourly ozone concentration values are added station-wise to obtain a typical ozone space distribution for the identified hours. For these identified hours, other meteorological parameters can be incorporated and their relation to ozone distributions interpreted.

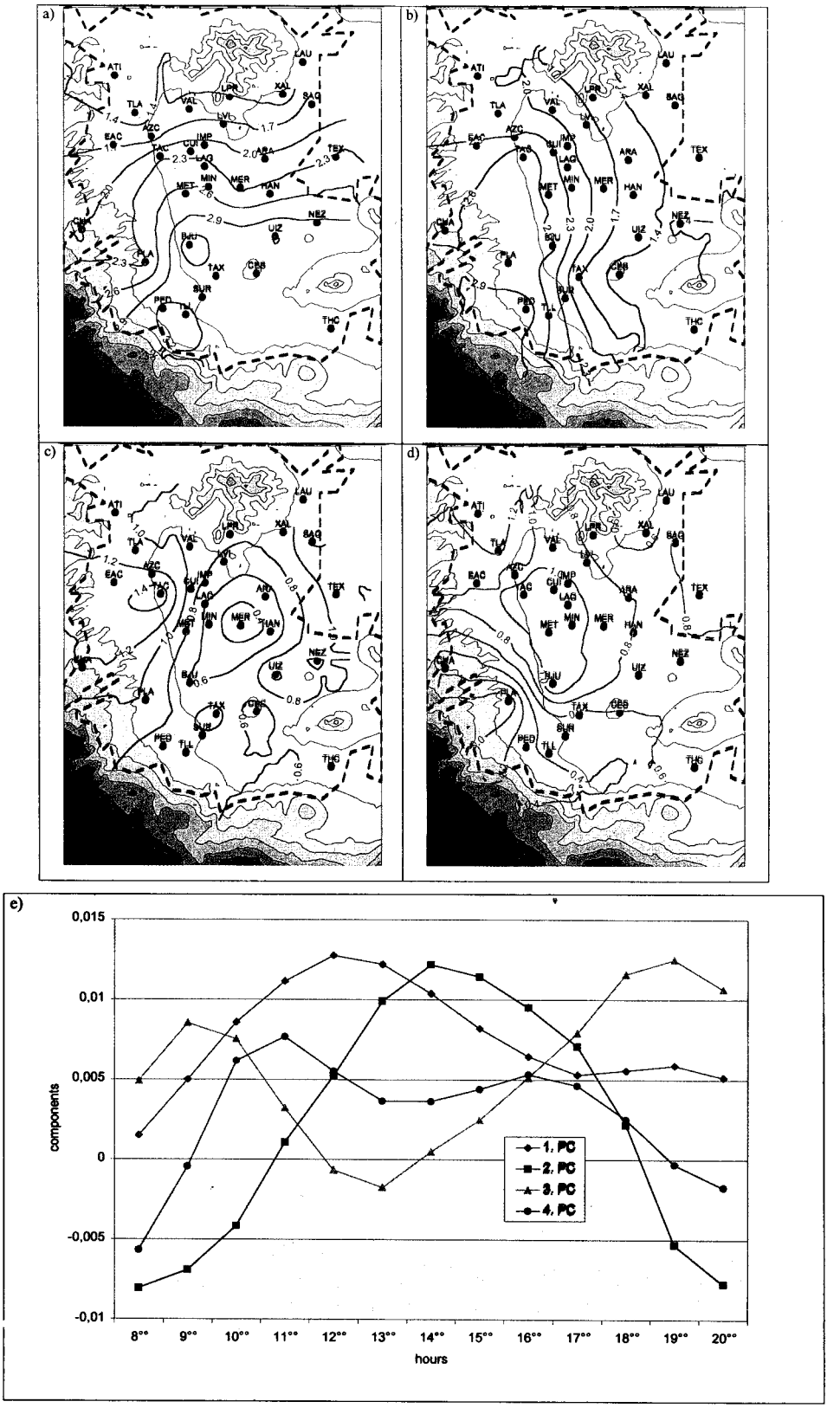

Fig. 4. Space patterns of the first four eigenvector coefficients (a-d) and the mean daily variation of the eigenvector components (e) extracted from the hourly ozone values from February to December 1995 (334 days) for 15 stations and from 8:00 to 20:00 hours. The first eigenvector explains 18.9%, the second 14.9%, the third 11.0% and the fourth 9.4%. Taken all together they explain 55.2% of the variance.

7. Types of space-time dynamics of ozone concentration in the MCMA and their origin

The first four principal components explain 54.2% of the total variance of the space ozone distribution between 8:00 and 20:00 hours in the area under study. The first one explains 18.9% already, the second 14.9%, the third 11.0% and the fourth 9.4%. That corresponding to the fifth eigenvector explains 7.0% and the sixth 6.4% of the total variance. Each of the following eigenvectors explains less than 5% of the total variance.

a) Space sample of the ozone concentration of the first eigenvector

Figures 5a and 5b show the mean distribution of those added ozone concentration hourly values for all stations in which the components of the first eigenvector are greater (Fig. 5a) or smaller than ± 1.5 sigma (Fig. 5b). The ozone distributions shown in Figures 5a and 5b are inverse (Skaggs, 1975; Bortz, 1994) and correspond very well to the space pattern of the first principal component coefficients illustrated in Figure 4a.

Figure 5a shows an ozone distribution with a marked north to south gradient. While the mean ozone concentration is about 0.06 ppm to the north of the MCMA the corresponding values in the south are around 0.11ppm. Only at station Plateros (PLA) to the southwest ozone concentration is rather moderate: 0.08ppm. The ozone values to the south exceed in more than 50% of the time the standard of 0.11ppm. The mean ozone concentrations in the hours when the PC's are smaller than 1.5 sigma, show maximum values to the northwest of the MCMA (Fig. 5b) near stations TLA, AZC and TAC.

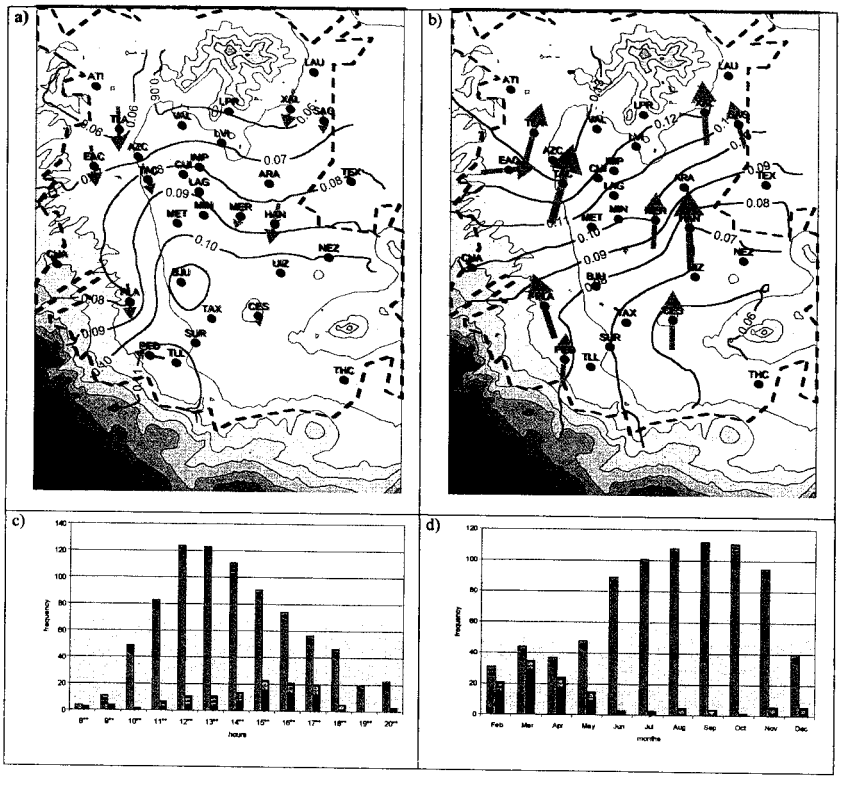

Fig. 5. (a-b) Mean ozone concentrations for those hours in which the values of the components of the first eigenvector are larger/smaller than 1,5 standard deviation (computed for the 4342 components of the first eigenvector). c) Number of hours in relation to the hour of the day in which the components of the first eigenvector are smaller/greater than 1.5 standard deviation. d) Number of hours according to the season in which the values of the components of the first eigenvector are larger/smaller than 1,5 standard deviation.

Figures 5c to 5d show the daily (5c) and annual cycle (5d) of the hourly frequencies of the occurrence of the spatial ozone distributions (types) shown in Figures 5a and 5b corresponding to component values of the first eigenvector greater or smaller than ± 1.5 sigma. Maximum daily frequencies for type 5a appear around 12.00-13.00 hours, for type 5b around 15:00-17:00 hours. The persistence of the types is described by the number of successive hours in which a type remains significant. For type 5a the persistence is valid for 32% of all hours in which this type is observed. For type 5b the persistence is smaller than 10%. The differences in the seasonal frequencies of type 5a and 5b allow a daily change between them only during the dry season since type 5a dominates from June to November and type 5b only during the dry season. Since the first PC comprises almost 20% of the explained variance, both ozone distributions may be considered very significant for the MCMA.

For the mean conditions it may be said with limitations that there is a close relationship between wind direction and the distribution of ozone in the MCMA. A large number of studies have shown the dependence of ozone distribution on direction of wind flow in the Mexico basin (Fast and Zhong, 1998a; Raga and Lemoyne, 1996; Whiteman *et al.*, 2000; Klaus *et al.*, 1988; Samson, 1978).

Type 5a shows high ozone concentrations at the south of the basin. The mean wind direction during the occurrence of type 5a is for all stations except Pedregal (PED) northerly (Fig. 5a). The winds from the east prevailing at Pedregal station favor the accumulation of ozone near this site. In addition the prevailing winds from the north favor high concentration of ozone and other pollutants at the southwest corner of the basin. Moreover, the upslope winds are important in the transport of these pollutants to higher levels where they are returned by the dominant upper-level south and southwest synoptic winds to the center of the basin where they are brought down through vertical diffusion to lower levels (Fast and Zhong, 1998a; Bossert, 1997). The northward spread of the area marked by high ozone concentrations in Figure 5a may be an indicator of this vertical diffusion processes.

The prevailing wind corresponding to type 5b blows very strong at all stations from the south quadrant (Fig. 5b). Therefore, the air pollutants are carried in a south to north direction favoring the accumulation of ozone on the northern quarters of the city. The south wind current on the east of the basin is the result of the thermally driven strong gap wind system dominating in late afternoon. These south winds overcome in the case of the occurrence of type 5b the whole Ajusco range in such a way that the strong thermal winds from the south dominate the whole basin. Consequently, a convergence zone results from this thermal south current and the thermal north wind usually dominating north of the city. If the south winds are limited to the eastern portion of the basin north winds can prevail on the western portion. The result from both wind systems is a converging cyclonic circulation in the late afternoon hours above the MCMA (Klaus *et al.*, 1999).

In all hours after 10:00 temperatures at Minería (MIN) and Texcoco (TEX) linked to type 5b remain 2-3°C above those corresponding to type 5a. It may be concluded that the area of maximum ozone concentration on the north (Fig. 5b), is related to a marked rise of the mean temperatures in particular during the late afternoon hours in the Mexico basin. Also solar radiation is relevant to the formation of ozone, especially during the wet season. The mixing of ozone with other pollutants reduces the intensity of solar radiation in the central parts of the urban area to a maximum of 25-35% when weak winds and high noon relative humidities prevail. (Jáuregui and Luyando, 1997). An analysis of global radiation values related to types 5a, b shows for stations Minería (downtown) and Texcoco (rural) an attenuation of around 250 W/m^2. In the late afternoon the irradiation values corresponding to type 5b are 100 W/m^2 at Texcoco and 70 W/m^2 at Minería higher than those observed in correspondence with type 5a. The possible cause for these contrasts in global radiation is the increase in cloudiness during the rainy season when type 5a reaches its maximum frequency.

b) Ozone distribution corresponding to the second eigenvector

The mean ozone distribution related to the second eigenvector estimated on the basis of the components smaller or larger than ± 1,5 sigma are shown in Figure 6a, 6b. Both distributions show a clear east/west

gradient differing each other clearly from those of the first eigenvector (Fig. 5a, 5b). The mean ozone concentration lies around 0.14 ppm (Fig. 6a) clearly surpassing the hourly standard.

Maximum values of ozone observed on the west and southwest of the city decrease toward the east reaching at Xalostoc (XAL) to the northeast and to the southeast at Cerro de la Estrella (CES) ozone values that are only half those observed at Pedregal (PED) station to the southwest (Fig. 6a). The inverse ozone distribution (Fig. 6b) shows highest concentrations toward the eastern portion of the MCMA. The highest mean values (around 0.05 ppm) remain clearly below the ozone standard while the lowest concentrations on the west portion of the MCMA are of the order of 0.024 ppm.

Maximum frequency of type 6a occurs at 14:00 hours (Fig. 6c), while the minimum are observed around 9:00 and 20:00 hours. In contrast with these daily behavior the frequency of type 6b shows a maximum during the morning and evening and a minimum at around noontime. Season wise type 6a shows maximum frequency in February and December. In this way type 6a is differentiated from that shown in Figure 5a (where high ozone concentrations on the southwest of the basin are observed) with maximum frequency in the wet period (Figs. 5d, 6d). Type 6b with maximum values on the east of the MCMA reaches maximum frequency during the wet season, especially in September.

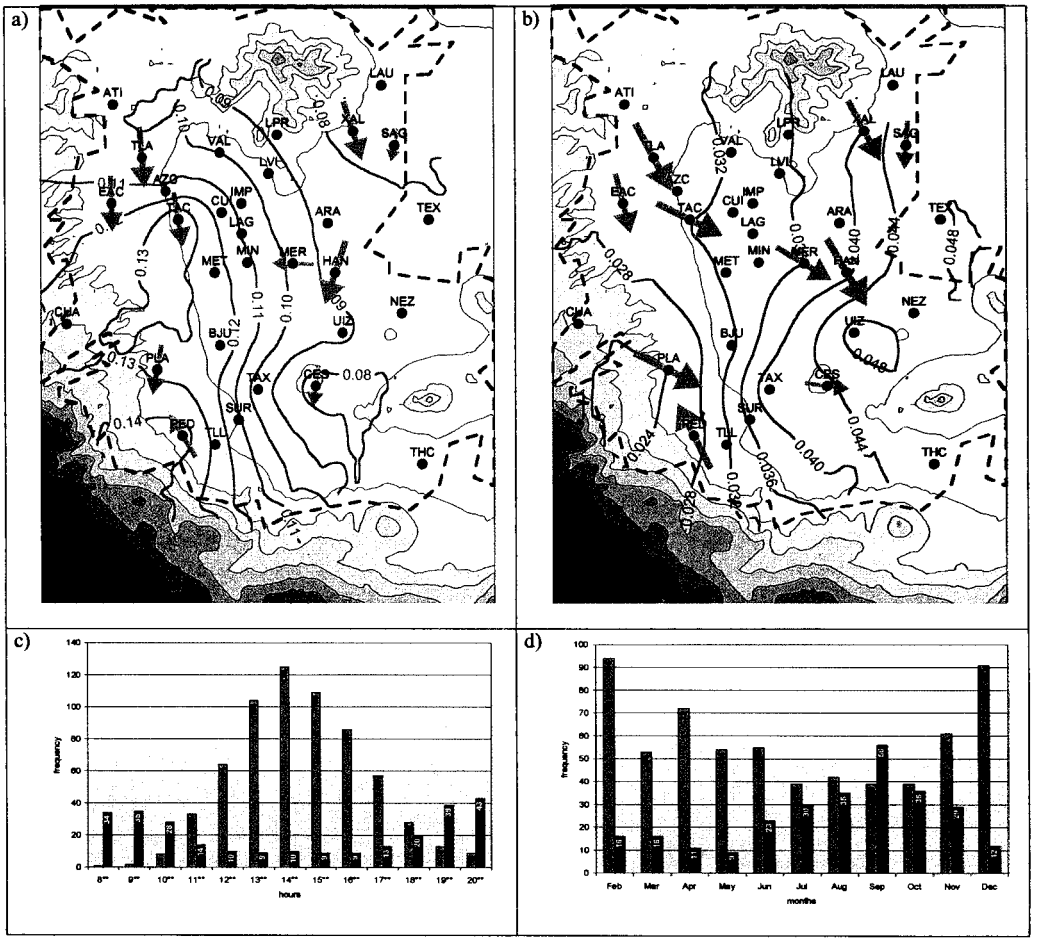

Fig. 6. (a-b) Mean ozone concentrations for the hours in which the values of the second eigenvector components are larger/smaller than 1,5 standard deviation (computed for the 4342 components of the second eigenvector). c) Number of hours in relation to the season in which values of the second eigenvector component are larger/smaller than 1,5 standard deviation. d) Number of hours according to the season in which the values of the components of the second eigenvector are larger/smaller than 1,5 standard deviation.

Type 6a persists 33 percent of all hours, type 6b only 13.5%. A change between these two types can only be rarely expected during the dry season, but more possibly during the wet period (Fig. 6d). The mean wind direction occurring in the hours of occurrence of type 6a shows that maximum ozone concentrations on the southwest are linked to winds from the north and northeast (Fig. 6a). These surface northerly winds are often linked to an upper south current. Air pollutants are carried by near-surface level winds from the north toward the high slopes of the mountains to the south. Here they are transported upwards and back by the upper south winds to the MCMA. This transport of pollutants from above through vertical diffusion may be evidenced by the southwesterly surface winds observed at Pedregal (PED).

On the eastern side of the basin maximum ozone concentration occurs in connection with type 6b. This pattern shows maximum frequencies during the night and morning hours of the wet season (Figs. 6c, 6d) related to ozone values between 0.03 and 0.05 ppm. Rainfall amounts in the Mexico basin increase from the northeast to the southwest (Klaus *et al.*, 1999; Jáuregui, 1996). Precipitation from convective clouds occurs in the MCMA during the afternoon and early night hours. The lower ozone concentration on the west side of the basin as compared to the east side is probably due to the washout effect. This hypothesis gets support in relation to pattern 6b and the daily course of temperature. Mean temperatures during the afternoon hours are some 4°C higher when type 6a prevails with respect to those linked to type 6b. The marked temperature difference may be explained by the cooling process linked to the higher cloudiness and rainfall on the west side of the basin. Global radiation values at stations Minería and Texcoco related to patterns 6a and 6b also explain increasing cloudiness during the afternoon hours related to type 6b.

A change from type 6a to 6b and vice versa is rarely observed. On the other hand the transition of type 5a to type 6a occurs in 8.4 percent of all hours. These transitions are concentrated in the rainy season months. The transition of type 6a to type 5a occurs only in 6.2% of all hours mainly during the rainy season months.

c) Ozone distribution corresponding to the third eigenvector

The third eigenvector explains 11% of the total variance. The ozone distribution corresponding to the third eigenvector has a multiple structure (Figs. 7a, 7b). The mean ozone concentration remains smaller by a factor of two to three than the mean concentration related to both first eigenvectors. Type 7a persists in 32% of the hours, type 7b in only 13%.

Lowest concentrations occur in downtown at station Merced (MER). They increase toward the perimeter of the city (Fig. 7a). When averaged over the hours in which the components of the third eigenvector are smaller than 1,5 sigma the highest concentrations are observed in downtown and to the south of the basin, whereas the smallest lies on the outskirts (Fig. 7b). The daily frequency distribution of type 7a is maximum during the morning and night hours, while at around noon hours they reach minimum values. The inverse type 7b shows a maximum frequency at around noon hours and two secondary maxima in the morning and night hours (Fig. 7c).

Type 7a displays a large seasonal variation (Fig. 7d). Maximum values occur in May, October, November and December. Type 7a seems to be representative of transition months between the rainy season and the dry season e.g. May and October. The inverse type 7b reaches only a small frequency maximum during the rainy season. Frequency values remain so small that this pattern is scarcely relevant.

Wind directions related to type 7a show in the mean on the west side of the basin strong northwest to west directions, while those stations on the east of the basin show strong winds from the east quadrant. The relatively strong winds may explain the low ozone concentrations observed in the basin. The high frequency of type 7a during night hours may be explained by the convergence between the east winds and the west north west winds. This convergence in the center of the urban area is reinforced by the nocturnal heat island (Klaus *et al.*, 1999; Jáuregui, 1997). The converging air masses carry pollutants toward downtown where they are lifted to higher levels. Of particular importance is the accumulation of nitrogen oxides downtown leading to a quick decrease of the ozone concentration (Höhlein *et al.*, 1996). On the outskirts of the city this destruction process takes place at a slower rate due to lower NO concentrations. As a result of this processes ozone concentrations remain low in downtown and high toward the perimeter until early morning.

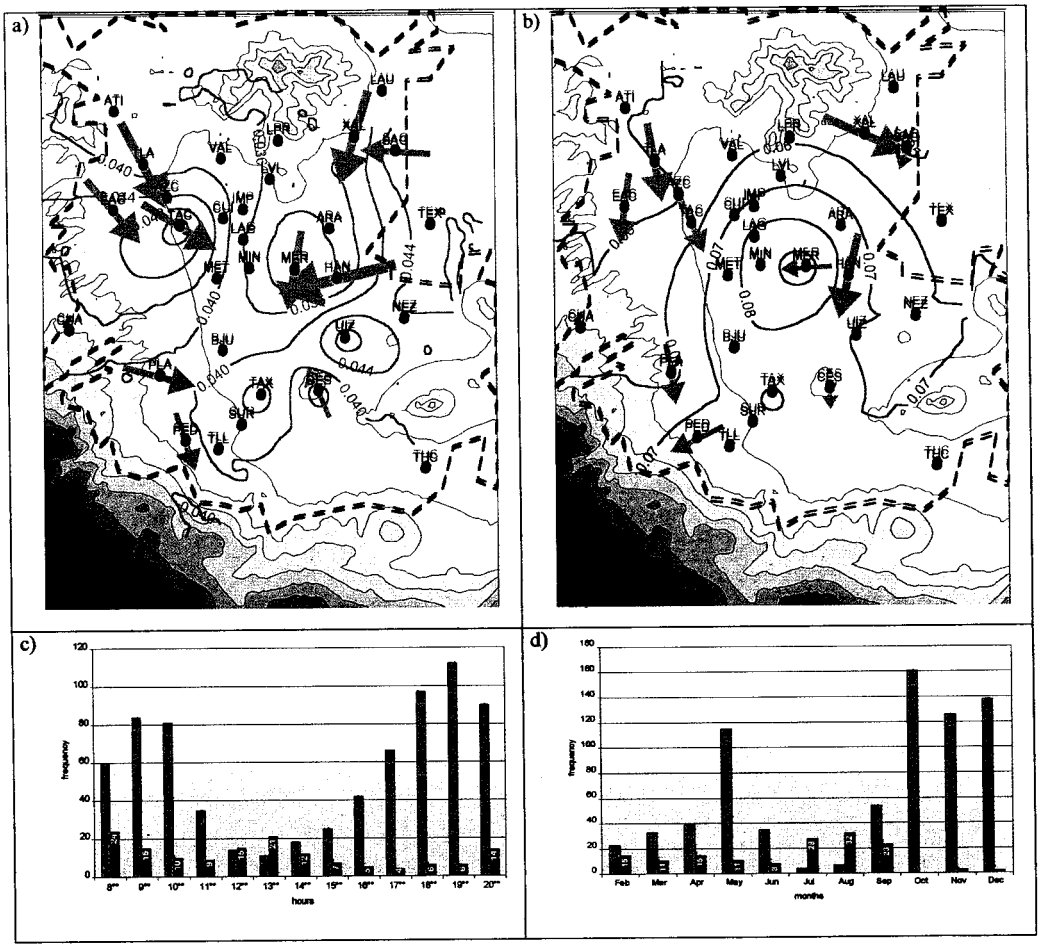

Fig. 7. (a-b) Mean ozone concentration for hours in which values of the components of the third eigenvector are greater/smaller than 1,5 standard deviation. (Computed for the 4342 components of the third eigenvector). c) Number of hours in relation to the time of the day in which values of the components of the third eigenvector are larger/smaller than 1,5 standard deviation. d) Number of hours in relation to the season in which values of the components of the third eigenvector were greater/smaller than 1,5 standard deviation.

Pattern 7b is rather infrequent. Frequency maximums are observed day and night (Fig. 7c). Extreme ozone concentrations in downtown with values of up to 0.18 ppm are observed between 12:00-13:00 hours. When averaged over the whole hours in which type 7b appears then these peaks disappear. Until 14:00 hours winds from the northern quadrant prevail in all stations that are at the origin of pollutant accumulation in the city center and on the south. Characteristic of type 7b is that the high pollution levels in downtown are isolated and not related to high ozone concentrations in the southwest portion of the basin like in the case of types 5a and 6a. A reason for this singularity seems to be the strong east to northeast wind related to type 7b at Merced. Simultaneously with type 5a light north winds prevail at Merced, with type 6a all winds in the MCMA are light (Figs. 5a, 6a).

Very high morning and noon temperatures and radiation values are related to type 7b resulting in extreme ozone values in the central parts of the MCMA. Type 7a occurs in connection with relatively low noon and afternoon temperatures and radiation values. As a result of the low available radiation energy the ozone production in the central quarters remains low.

d) Ozone distribution corresponding to the fourth eigenvector

The space distribution of ozone related to the fourth eigenvector (Fig. 8a) shows maximum ozone values to the west of downtown at station Tacuba (TAC) and minimum at Plateros (PLA). Type 8a shows maximum frequency around 11:00 and 16:00 hours (Fig. 8c). Maximum frequencies occur during the wet season. (Fig. 8d).

Figure 8e shows hourly wind directions and velocities linked to type 8a. Winds from the northwest are dominant on the west side of the basin during all day while northeasterlies prevail on the east side. Only at Pedregal and Merced winds are variable while on the rest of the network they show a marked persistence. Wind direction changes cannot therefore explain pattern 8a. Since type 8a reaches a maximum frequency during the wet season, it is likely that the higher cloudiness and rainfall on the west prevents ozone formation there shifting the maximum ozone concentration further to the east.

The inverse ozone distribution (type 8b in Fig. 8b) shows the highest concentration at Plateros (PLA) and minimum at Tlanepantla (TLA) and Xalostoc (XAL). Type 8b is very frequent in the morning and night hours, with a secondary maximum at around 13:00 hours. Type 8b is almost exclusive of the dry season with maximum frequency in March (Fig. 8d). Figure 8f illustrates the connection of type 8b with the mean wind vectors as well as with the mean hourly ozone concentrations which are > 0.15 ppm during 12:00-16:00 hours at Plateros (PLA) and Pedregal. At stations Cerro Estrella (CES) and Hangares (HAN) concentrations above 0.11 ppm occur at 12:00 and 16:00 hours and at Merced (MER) from 12:00 to 16:00 hours. Extreme ozone concentration may occur in almost all other monitoring stations at about noontime with pattern 8b.

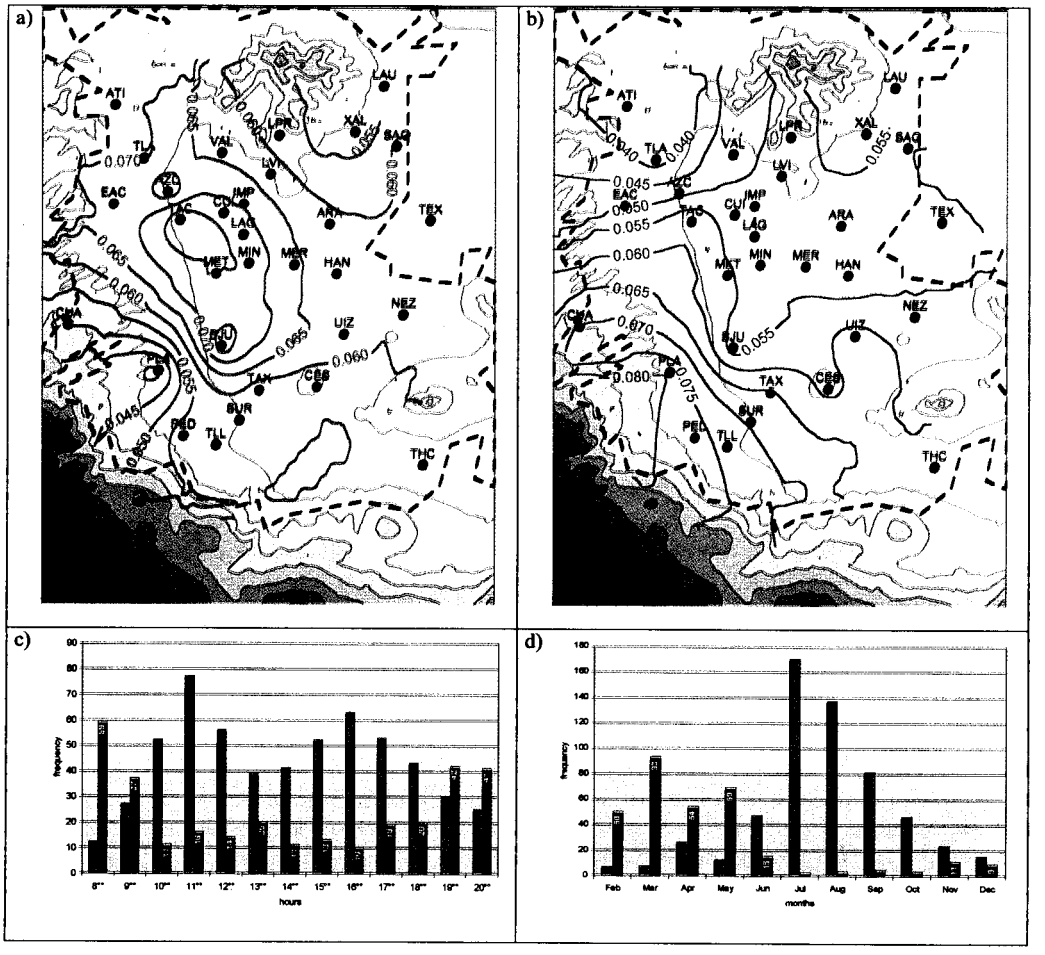

Fig. 8.

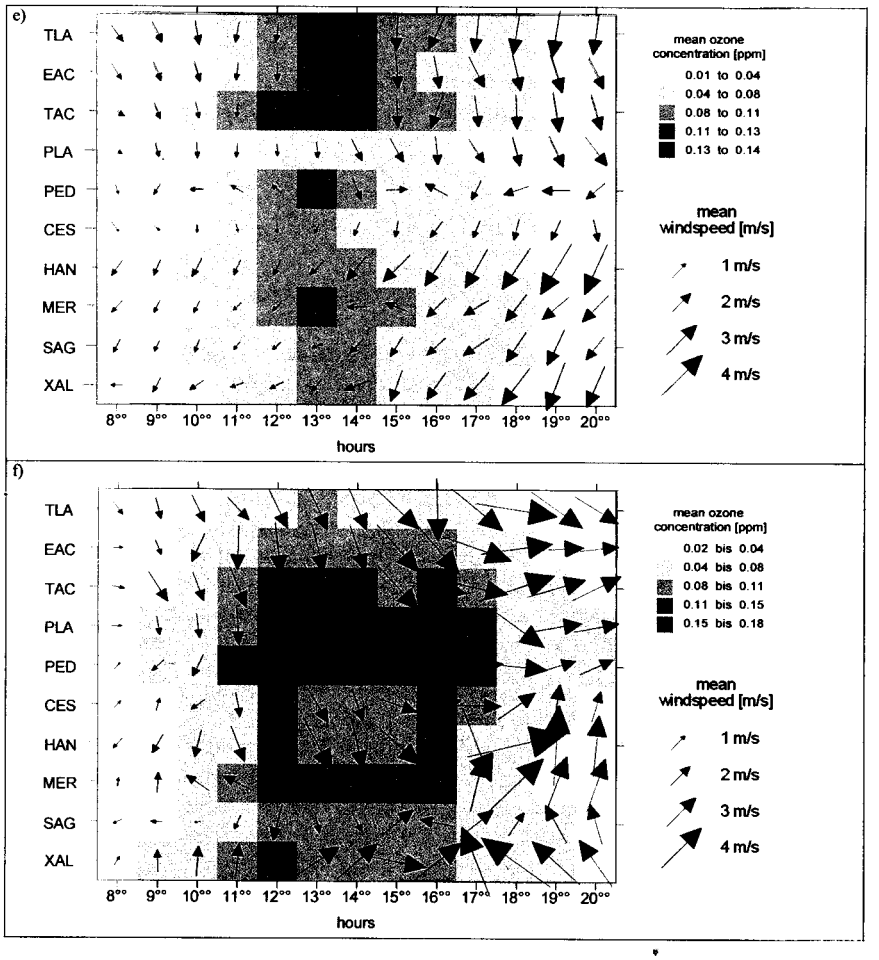

Fig. 8. (a-b) Mean ozone concentration for hours in which values of the components of the fourth eigenvector were greater/smaller than 1,5 standard deviation (computed for 4342 components of the fourth eigenvector). c) Number of hours in relation to the time of day in which values of components of the fourth eigenvector were greater/smaller than 1,5 standard deviation. d) Number of hours in relation to time of day in which values of the components of the fourth eigenvector were greater/smaller than 1,5 standard deviation. (e-f) Mean wind direction, wind velocity and mean ozone concentration for the hours in which the value of the fourth eigenvector is greater/smaller than 1,5 standard deviation.

At around 15:00 hours (except stations Merced and Xalostoc) strong winds from the north to northwest are observed. (Fig. 8f). Southeast winds prevail at Merced and from the southwest at Xalostoc until 16:00 hours. From 16:00 hours on the eastern portion of the basin the thermal southerly winds prevail while on the west the dominant winds blow from the northwest and west reaching up to 4m/s. The north wind current may explain the high ozone concentrations observed on the southwest portion of the basin. Since the strong north winds are the most frequent in the Mexico basin they may clearly explain by themselves the not infrequent high ozone concentrations observed at many stations in this part of the basin.

From the daily temperature course it may be inferred that the highest temperatures occur at about 16:00 hours with type 8b simultaneous with the establishment of the thermal southerly winds. Maximum irradiation occurs in relation to type 8b at 13:00 hours. The highest mean hourly values of global radiation observed in 1995 occur in connection with type 8b and reach at Texcoco 920 W/m^2 and at Minería 700 W/m^2. This means that the high ozone concentrations observed from 12:00 to 16:00 hours in the large area of the central and southwestern sectors of the basin may be the result of high irradiation levels. Moreover

the extreme ozone concentrations related to type 8b at noon hours seem to be completely unrelated to conditions observed on the previous day. Global radiation maximum values of 790 W/m^2 and 540 W/m^2 at Texcoco and Minería respectively, are related to type 8a. As mentioned before, light cloud cover may explain the limited extent of high ozone concentration at Tacubaya (TAC) in connection with the occurrence of type 8a.

8. Discussion and outlook

Patterns of ozone concentration are examined by means of the first four eigenvectors. Using this approach almost half (54,2%) of the total variance of the space-time variations of ozone concentrations may be explained. This has been accomplished by using a simple model of circulation and stability conditions in the Mexico basin. The dominant winds favour pollutant accumulation on the windward side of the surrounding mountains. As a consequence the highest ozone concentrations are observed there. Ozone accumulation is evident not only at the mountain slopes but also on the transport track. This can be documented by the coincidence of maximum ozone concentrations with areas of strong confluence or with areas of convergence resulting from changes in wind speed. These areas are found in the central parts of the city and where the northwest winds on the west side of the basin converge with the easterly, southeasterly and southerly winds on the east portion of the basin. This converging zone is frequently related to a cyclonic circulation. The precise location of the vortex depends on the intensity of the interaction between the local and regional wind systems. A significant relationship between the extracted space patterns and the time/space variations of wind velocity could not be shown from the 1995 data.

During the dry season some of the spatial pattern of the ozone concentration may be explained by the downward diffusion of upper highly polluted air. Fast and Zhong (1998 a, b) have developed a mesoscale circulation and stability model for the Mexico basin in which the strong upslope winds feed the heavily polluted air into the upper air stream. Especially when west and southwesterly upper winds are prevailing the highly polluted air mass is returned over the basin and from thereon through vertical diffusion processes carried downward to lower levels. The present study with data from 1995 gives support to the Fast and Zhong model (1998a, b).

The extracted patterns of the typical ozone distribution can in connection with proposed circulation structures, contribute to the knowledge of pollution prognosis. Results presented in this study are valid only for year 1995; a further extension of analysis is required. However, the main results from the present study will remain valid. Relationships between the upper level wind directions and intensities should be more marked than those obtained in this work.

Findings from Whiteman *et al.* (2000) and from Fast and Zhong (1998 a, b) as well as those derived from the present study give an insight into the relationship between meteorological parameters and ozone distributions. Work in the modelling and analysis of the data will allow further knowledge in the dynamics and relevant processes taking place in the MCMA.

Acknowledgements

We would like to thank Ms. Ma Esther Grijalva, Ms. Thelma del Cid and Elda Luyando for helping in the preparation of the manuscript in its final form.

REFERENCES

Beceiro-Gonzalez, E., J. M. Andrade, E. Serrano, P. López and D. Prada, 1998. Characterization of anthropohenic and natural emissions of particulate heavy metals in La Corona. *Afinidad,* Vol. **55**, No. 475, pp. 207-212.

Bliford, I. H. and G. O. Meeker, 1967. A factor analysis model of large scale pollution. *Atmos. Environment*, Vol. **1**, pp. 147-157.

Bortz, J., 1994. Statistik für Sozialwissenschaftler. 4. Aufl. Springer Verlag.

Bossert, J. E., 1997. An investigation of flow regimes affecting the Mexico City Region. *Journal of Applied Meteorology*, Vol. **36**, No. 2, pp. 119-140.

Cevallos, D., 1998. Environment-Mexico: Longer Commutes and Higher Pollution Levels. Inter Press Service, April 1998. under www.oneworld.org/ips2/apr98/20_47_077.html (13.6.1999).

Collins, C. H. O. and S. T. L. Scott, 1993. Air Pollution in the valley of Mexico City. *The Geographical Review*, Vol. **83**, No. 2, pp. 119-133.

D. G. P. C. C., 1995. Mexico City - Direction for Pollution Prevention and Control D. G. P. C. C. unter www.sima.com.mx/sima/df/dfeng.html (13.6.1999).

Doran, J. C. and S. Zhong, 1999. Thermally driven gap winds into the Mexico City Basin. Reprint of a paper submitted to *Journ. of Appl. Meteorol.* (20.10.1999).

Ezcurra E. and M. Mazari-Hiriarti, 1996. Mexico City: Metaphor for the World's Urban Future. *Environment*, Jan-Feb. pp. 6-33.

Fast, J. D. and S. Zhong, 1998a. Meteorological factors associated with inhomogenous ozone concentrations within the Mexico City basin. *Journal of Geophysical Research*, Vol. **103**, No. D15, pp. 18927-18946.

Fast, J. D. and S. Zhong, 1998b. Mexico City Modeling Studies. under www.pnl.gov/ atmos_science/as_meso5.html (13.6.1999).

Harrison, S. H., 1997. Regression modeling of hourly No_x and NO_2 concentrations in urban air in London. *Atmos. Environment*, Vol. **31**, No. 24, pp. 4081-4094.

Höhlein, B., P. Biedermann, D. Klemp and H. Geiß, 1996. Verkehrsemissionen und Sommersmog, Jülich, 1996.

Jáuregui, E. and E. Luyando, 1997. Global radiation attenuation by air pollution and its effects on the thermal climate in Mexico City. *Int. J. of Climatology*, Vol. **19**, pp. 683-694.

Jáuregui, E. and E. Romales, 1996. Urban effects on convective precipitation in Mexico City. *Atmos. Environment*, Vol. **30**, No. 20, 3383-3389.

Jáuregui, E., 1997. Heat Island development in Mexico City. *Atmospheric Environment,* Vol. **31**, No. 22, pp. 3821-3831.

Jáuregui, E. and A. Tejeda, 1997. Urban-Rural humidity contrast in Mexico City. *Intern. Journ. of Climatology*, Vol. **17**, pp. 187-196.

Klaus, D., W. Lauer and E. Jáuregui, 1988. Schadstoffbelastung und Stadtklima in Mexiko-Stadt. In: Akademie der Wissenschaften und der Literatur.

Klaus, D., E. Jáuregui, A. Poth, G. Stein and M. Voß, 1999. Regular circulation structures in the tropical basin of Mexico City as a consequence of the urban heat island effect. *Erdkunde*, Vol **53**, pp. 231-243.

Lam, K. C. and S. Q. Chen, 1998. A synoptic climatological approach to forecast concentrations of SO_2 and NOx in Hong Kong. *Environmental Pollution*, Vol. **101**, No. 2. pp. 183-191.

Newell, E. R., J. W. Kidson, D. G. Vincent and G. J. Boer, 1972. The General Circulation of the tropical Atmosphere and the interactions with extratropical latitudes. Massachusetts Institute of Technology. Baskerville, USA.

Nickerson, E. C., G. Sosa, H. Hochstein, P. Mc Caslin, W. Luke and A. Schanot, 1992. Project AGUILA: *in situ* measurements of Mexico City air pollution by a research aircraft. *Atmospheric Environment* Part B: Urban Atmosphere, **26B**, 445-452.

Oke, T. R., R. A. Spronken, E. Jáuregui and C. S. B. Grimmond, 1999. The energy balance of central Mexico City during the dry season. *Atmos. Environment*, Vol. **33**, pp. 3919-3930.

Peterson, J. T., 1970. Distribution of sulphur dioxide over St. Louis as described by empirical eigenvectors and its relation to meteorological parameters. *Atmos. Environment,* Vol. **4**, pp. 501-518.

Peterson, J. T., 1972. Calculation of sulphur dioxide concentrations over St. Luis. *Atmos. Environment*, Vol. **6**, pp. 433-442.

Raga, G. and L. Lemoyne, 1996. On the nature of air pollutant dynamics in Mexico City. Part I: A non-linear analysis. *Atmos. Environment.* Vol. **30**, pp. 3987-3993.

Samson, P. J., 1978. Noctural Ozone Maxima. *Atmospheric Environment*, Vol. **12**, pp. 951-955.

Skaggs, R. H., 1975. Drought in the United States, 1931-1940. *Annals of the Association of American Geographers*, **63**. 391-402.

Smith, J., 2000. Little by little, breathing easier in Mexico City. Los Angeles Times, January 15, p. A2.

Statheropoulos M., N. Vassiliadis, and A. Pappo, 1998. Principal component and canonical correlation analysis for examining air pollution and meteorological data. *Atmos. Environment*, Vol. **31**, No. 6, pp. 1087-1095.

Whiteman, C. D., S. Zhong, X. Bian, J. D. Fast and J. C. Doran, 2000. Boundary Layer Evolution and Regional-Scale Diurnal Circulations over the Mexico Basin and Mexican Plateau. *Journal of Geophysical Research-Atmosphere,* Vol. **108**, No. D8, pp. 10081- 10102.

Williams, M. D., M. J. Brown, X. Cruz, G. Sosa and G. Streit, 1995. Development and testing of meteorology and air dispersion models for Mexico City. *Atmos. Environment*, Vol. **29**, No. 21, pp. 2929-2960.

WHO, 1997. WHO guidelines for air quality. Fact Sheet N°187, December 1997.